

Structure and magnetism in CePt_{2+x}

J. M. Lawrence and Y.-C. Chen
University of California, Irvine, California 92697-4575

G. H. Kwei
Lawrence Livermore National Laboratory, Livermore, California 94550

M. F. Hundley and J. D. Thompson
Los Alamos National Laboratory, Los Alamos, New Mexico 87545
 (Received 3 September 1996)

Neutron diffraction results for CePt_{2+x} alloys with $0 \leq x \leq 1$, combined with low resolution room temperature x-ray diffraction and electron microscopy, confirm that the alloys are single phase. The data can be fit for all x with nearly equal agreement factors by structural refinements in either the *C15* (MgCu_2) phase or the *C15b* (AuBe_5) structure. Observation of small peaks in the diffraction pattern for CePt_3 that are forbidden in *C15* suggest that *C15b* is the correct structure for this composition (and possibly for the other alloy compositions); and application of Hamilton's test indicates that the *C15b* structure is preferred over the *C15* to the 95% confidence level. Magnetic susceptibility and specific heat measurements indicate that the cerium is essentially localized and trivalent for all x . The antiferromagnetism observed for CePt_2 may be absent in the alloys, which behave as typical nonmagnetic cerium heavy fermion compounds with Kondo temperature $T_K \approx 2$ K. [S0163-1829(97)04225-2]

CePt_2 is a cubic compound that grows in the *C15* (MgCu_2) Laves phase.¹ It orders antiferromagnetically at $T_N = 1.6$ K and the specific heat and susceptibility are as expected for localized trivalent cerium, where the $J = 5/2$ moment is split by a cubic crystal field.² Based on low resolution x-ray measurements and metallography,¹ it has been reported that CePt_2 has an extraordinarily large homogeneity range, i.e., the alloys CePt_{2+x} grow in the *C15* structure for $0 \leq x \leq 1$. Recently it has been reported³ that ultrathin films of CePt_{2+x} crystallize via solid state diffusion of Ce on the Pt(111) surface; the measured stoichiometry was $\text{CePt}_{2.2}$. Photoemission experiments performed on these films gave evidence for dispersion of the $4f$ levels.⁴ Such dispersion might be expected for strongly mixed-valent cerium compounds and Ce $3d$ core-level (XPS) in both the ultrathin films³ and in bulk samples⁵ of CePt_3 give evidence for mixed valence. As further background to these studies of the crystalline films, we have undertaken a new study of bulk samples of CePt_{2+x} alloys. One purpose is to better determine the structure by performing Rietveld refinement using neutron diffraction data. A second purpose is to determine whether the susceptibility and specific heat measurements give any evidence that the $4f$ electron is strongly mixed valent in the alloys for $x \neq 0$, which might help explain the photoemission results.

The samples were manufactured by arc melting, using high purity Pt and Ce obtained from Johnson Matthey and the Ames Laboratory, respectively. Samples were annealed for periods of 16–40 h at either 1200 or 1370 K. Low resolution room temperature x-ray diffraction data were collected using a Rigaku Miniflex system. The results were in good agreement with the older work;¹ in particular, all diffraction peaks could be indexed using the *C15* structure, with lattice

constants (Table I) decreasing linearly by about 1% with increasing x . There was no evidence of Pt segregation. Minor impurity peaks indicated the presence of a small (<5%) amount of a second phase; these peaks did not correspond to any known Ce/Pt compound or oxide. The samples were examined using an ISI SR-50A scanning electron microscope; an image of CePt_3 at a magnification of 300 is shown in Fig. 1. Large facets of linear dimensions $100 \mu\text{m}$ indicate that the sample is well crystallized. For samples at other values of alloy concentration x , the facets were somewhat smaller. The stoichiometry inside a $1 \mu\text{m}$ focal area within different facets was measured with an HNU 5000 system via energy dispersive x-ray analysis (EDX) using the Ce and Pt fluorescent L x-ray lines excited by 20 keV electrons. The stoichiometry measured in this fashion is uncertain by 10%; nevertheless, the results (Table I) are in good overall agreement with the expected stoichiometries.

For the neutron diffraction studies, 5 g samples were powdered and annealed at 770 K for 12 h. These were loaded in V tubes, and mounted on the General Purpose Powder Diffractometer (GPPD) at the Intense Pulsed Neutron Source (IPNS) at Argonne National Laboratory. The samples were cooled by a closed-cycle helium refrigerator; the temperature was held at 13 K. Data were collected in the $\pm 60^\circ$, $\pm 90^\circ$, and $\pm 150^\circ$ detector banks. Representative data for CePt_2 and CePt_3 are shown in Fig. 2.

We refined the structure of CePt_{2+x} using the GSAS software⁶ for Rietveld refinement, for two cases: the disordered *C15* structure (space group $Fd-3m$) where the extra Pt should alloy (randomly) onto all Ce sites, and the disordered *C15b* (AuBe_5) structure ($F-43m$). The latter is observed in compounds such as YbInCu_4 ⁷ where the Cu resides on the usual Cu sites of the MgCu_2 structure while the Yb and In separate onto the (0,0,0) and (1/4, 1/4, 1/4) Mg sites. It is a

TABLE I. The stoichiometries (Pt/Ce ratio) measured by EDX (*: powder samples), the room temperature lattice constants $a_0(300\text{ K})$ measured by low resolution x-ray diffraction, and the parameters of the fits to the neutron data for Rietveld refinements on the C15 and C15b structures [lattice constants $a_0(13\text{ K})$, isotropic displacement parameters U_{iso} on the Ce(1) (0,0,0) and Ce(2) (1/4, 1/4, 1/4) sites and on the Pt sites, and the reduced χ^2_{red} and R values). The left-hand column gives the stoichiometry based on the starting compositions prior to melting. Typical uncertainties are ± 0.2 – 0.3 for the EDX stoichiometry, ± 0.007 for $a_0(300\text{ K})$, ± 0.0002 for $a_0(13\text{ K})$, and ± 0.01 for $100*U_{\text{iso}}$.

	EDX (Pt/Ce)	$a_0(300\text{ K})$ (Å)	$a_0(13\text{ K})$ (Å)	$100*U_{\text{iso}}$ (Å ²)			χ^2_{red}	R_{wp} (%)
				Ce(1)	Ce(2)	Pt		
CePt _{2.00}	1.7*	7.745						
C15:			7.7172	0.40	0.40	0.27	2.22	6.86
CePt _{2.21}	2.1	7.734						
CePt _{2.26}								
C15:			7.6974	1.70	1.70	0.36	1.99	6.99
C15b:			7.6975	0.38	3.85	0.39	1.93	6.89
CePt _{2.50}	2.5	7.706						
C15:			7.6708	2.36	2.36	0.40	2.41	6.50
C15b:			7.6709	1.01	4.01	0.40	2.38	6.47
CePt _{3.00}	2.9, 3.2*	7.673						
C15:			7.6380	3.52	3.52	0.31	2.43	7.65
C15b:			7.6380	4.42	3.01	0.31	2.42	7.63

plausible alternative for CePt_{2+x}, where there is an appreciable size difference between Ce and Pt atoms (fcc radii of 1.82 and 1.39 Å, respectively). For this case we assume that all the (0,0,0) sites are fully occupied by Ce and that the remaining Ce and the extra Pt alloy randomly onto the (1/4, 1/4, 1/4) sites.

We constrained the site occupancies to give the expected stoichiometry; in addition to the lattice parameters and isotropic displacement parameters, we refined terms for the sample absorption, extinction and background as well as the strain-related term in the profile coefficients. The results are given in Table I, and fits to the data for CePt₂ and CePt₃ are shown in Fig. 2. For all $x > 0$ the calculated diffraction pattern for the C15b structure is very similar to that for the C15 structure on the scale of these plots. Both structures fit the data very well, with respectable values for the R factors and reduced χ^2 for all x . The deviations from the fit for $x \leq 0.5$ are very similar to that shown in Fig. 2(a) for CePt₂.

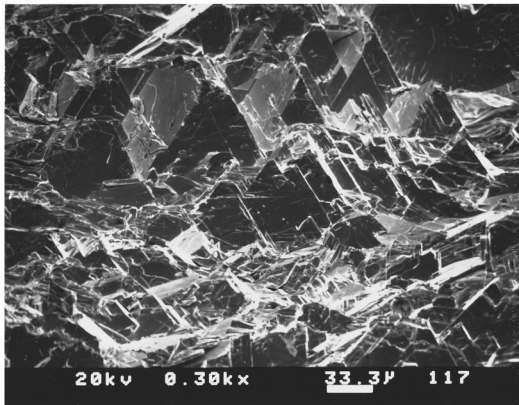


FIG. 1. Scanning electron microscope image of CePt₃ at a magnification of 300. The electron energy was 20 keV.

For CePt₃, the R values are somewhat larger and the deviations are visibly larger [Fig. 2(b)]. For $x \leq 0.5$ there is no evidence in the data for second phases, but for CePt₃ small impurity peaks near 2.125 and 2.329 Å are present in the data; these cannot be assigned to known structures such as Pt or CePt₅ (the impurity phases expected based on the equilibrium phase diagram). The diffraction lines do not broaden noticeably in the alloys; as a confirmation, we found that the strain-related parameter σ_1 of the profile coefficients did not vary significantly with x . The lattice parameter shows the same 1% linear decrease as x varies from 0 to 1 as mentioned above for the room temperature parameters. The isotropic displacement parameter for the Pt site is quite typical, but for the Ce site it increases from a typical value for CePt₂ to very large values for the alloys. Since the data were collected at 13 K, this represents groundstate displacement, i.e., Pt atoms occupying Ce sites are displaced slightly and randomly from the position mandated by symmetry.

While the fits are respectable for either case, the agreement factors are slightly smaller for the C15b structure. Certain reflections [viz. the (4,2,0) and (6,0,0)] which are forbidden in the C15 structure are allowed in the C15b. Unfortunately the predicted intensity in these peaks is small. Nevertheless, the inset in Fig. 2(b) shows a small peak at 1.710 Å, of the correct magnitude for the (4,2,0) reflection and similarly a slightly larger peak at 1.274 Å as expected for the (6,0,0) reflection appears as a shoulder to the more intense (5,3,1) peak at 1.293 Å. Although the scatter in the data and the existence of the small unassigned impurity peaks reduces the certainty of this assignment, the existence of these peaks suggests that CePt₃ (and possibly the other alloys as well) form in the disordered C15b structure. To corroborate this assignment we applied Hamilton's test. We refined the structure in the C15b space group with the Pt site constrained to (5/8, 5/8, 5/8) and with the isotropic displace-

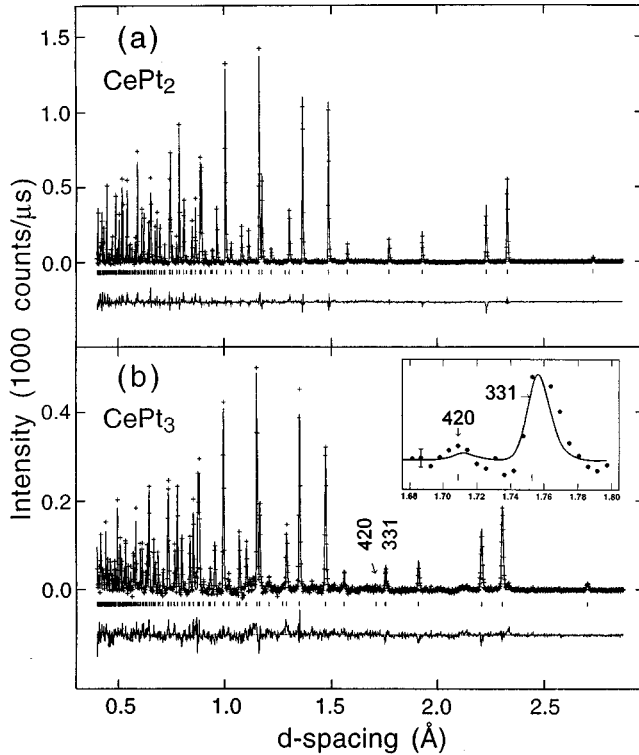


FIG. 2. Neutron diffraction data for (a) CePt_2 and (b) CePt_3 at $T=13$ K. The + marks are the observed profile (data); the line through the data is the calculated profile for the $C15$ structure in (a) and for the $C15b$ structure in (b). For the parameters of the refinement, see Table I. The lower curves in each case represent the difference between the observed and calculated profiles. The inset shows a blow up of the region near the $(4,2,0)$ reflection at 1.709 Å; this peak is forbidden in the $C15$ structure, but has a very small expected amplitude in the $C15b$ structure, as shown by the calculated profile. These data are from the 60° detector bank with averaging over three adjacent points. An example of the estimated error in each averaged data point is shown on the left-hand side.

ment factor for the “Ce” site constrained to 0.0040 Å², in keeping with the value for CePt_2 , and that for the Pt site constrained to 0.0035 Å², the average for CePt_{2+x} (see Table I). Under these constraints the two models (disordered $C15$ and disordered $C15b$) differ in only one degree of freedom. The agreement factors R_{wp} for the two cases were 8.77 and 8.73%, respectively. Although the change in agreement factors is small, the large number of data points results in a Hamilton’s \mathcal{R} -test that gives a 95% confidence level that the latter structure is preferable. When the “Ce” displacement parameter is constrained to a value 0.035 Å² consistent with the larger values observed for CePt_3 (Table I), the values of R_{wp} decrease and the Hamilton \mathcal{R} -test gives an even higher confidence level for the $C15b$ structure with preferential Pt occupancy on one of the Ce sites.

The susceptibility was measured for temperatures in the range 1.8–350 K using a Quantum Design SQUID (superconducting quantum interference device) magnetometer; typical results are shown in Fig. 3. The susceptibility of CePt_2 reproduces the earlier work² very well. It has a form characteristic of the susceptibility of other antiferromagnetic trivalent cerium compounds that are subject to cubic crystal

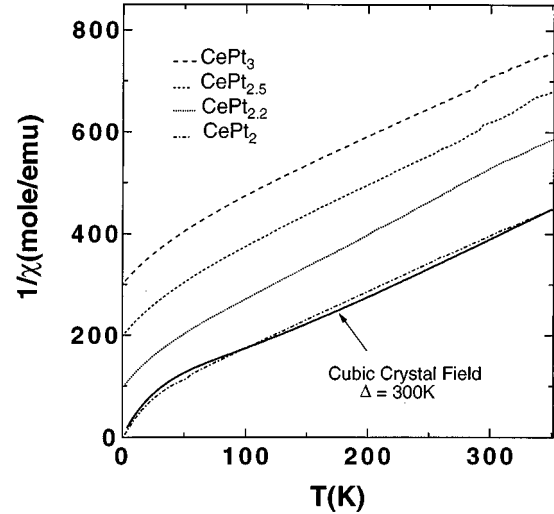


FIG. 3. The susceptibility, plotted as $1/\chi$ vs temperature, of CePt_2 and CePt_{2+x} alloys for $x=0.21, 0.50,$ and 1.00 . Successive curves for increasing alloy concentration x are offset by 100 mole/emu. The solid line represents the prediction for a $J=5/2$ moment split by $\Delta=300$ K in a cubic crystal field. The alloys have very similar susceptibilities to that of CePt_2 , indicating that the cerium is essentially trivalent.

fields. In the earlier work the susceptibility below 100 K could be fit assuming a crystal-field Γ_7 ground-state doublet separated by $\Delta=215$ K from the excited Γ_8 quartet. For our data a somewhat larger value ($\Delta=300$) K yields a reasonable fit (Fig. 3). The susceptibility of the CePt_{2+x} alloys is 25% larger at 20 K and 10% smaller at 350 K than that of CePt_2 , but otherwise is very similar. These changes could arise from a distribution of crystal-field splittings induced by the disorder in the Ce environment. In any case, the susceptibility of the alloys is very similar to that of CePt_2 , and very different from the small (≈ 0.001 emu/mole Ce) and weakly temperature dependent susceptibility expected for a strongly mixed valent compound. This suggests that the cerium remains essentially trivalent in the alloys.

The specific heat for the alloys for 1.2–20 K, measured using a thermal relaxation technique, is shown in Fig. 4. Below 10 K our data reproduce the earlier work² for CePt_2 reasonably well: a peak at $T_N=1.6$ K reflects the onset of antiferromagnetic order and the integrated entropy between 0 and 10 K is approximately $0.9R \ln 2$, implying that the ordering occurs for a Γ_7 ground-state doublet. We have extended the measurement to higher temperatures (20 K) than in the older measurement (9 K). Above 10 K the specific heat increases primarily due to thermal population of phonons; the phonon contribution, estimated from the coefficient of the T^3 term observed between 4 and 8 K in the earlier measurement² of LaPt_2 , is shown as a solid line in Fig. 4(a). The difference between the measured specific heat and this estimate of the phonon contribution is 2.6 J/mole K at $T=20$ K; if the Γ_7/Γ_8 crystal-field splitting were $\Delta=100$ K, the Schottky contribution would have this magnitude at 20 K. This value of Δ is qualitative, depending in detail on the magnitude of the phonon term and of the high-temperature tail of the peak at T_N . If the latter is significant at 20 K, the value of Δ required to fit the data would have to

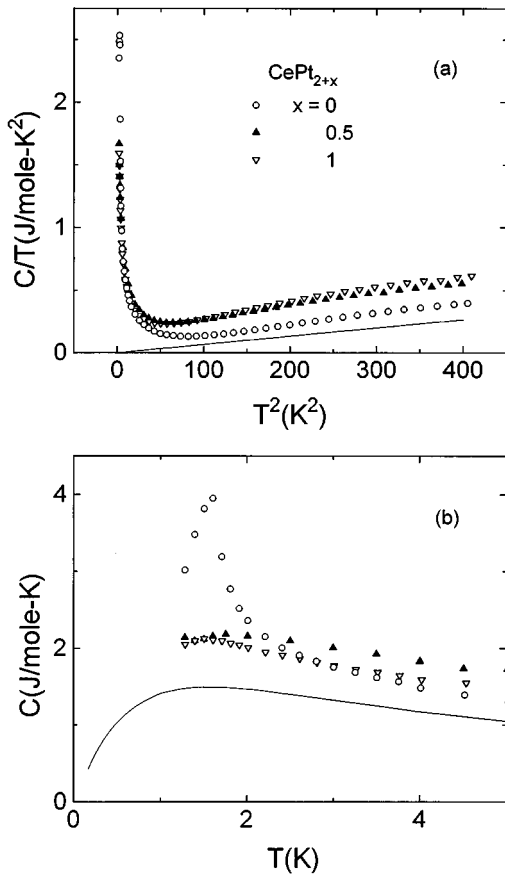


FIG. 4. The coefficient of specific heat $C(T)/T$ plotted versus the square of the temperature for CePt_2 , $\text{CePt}_{2.5}$, and CePt_3 . The solid line represents the expected phonon term, taken as equal to the T^{-3} term measured² in the interval 4–8 K for LaPt_2 . (b) The specific heat versus temperature for $1.2 < T < 5$ K. The sharp peak, due to antiferromagnetic order, observed for CePt_2 is not present for the alloys; the broadened peaks are similar to the prediction (solid line, from Ref. 8) of the $S=1/2$ Kondo model with Kondo temperature $T_K=1.5$ K.

be larger; in any case it is in order-of-magnitude agreement with the value (200–300 K) obtained from the susceptibility.

The specific heat of the CePt_{2+x} alloys is very similar to that of CePt_2 in the interval 2–5 K. Above 5 K the specific heat of the CePt_{2+x} alloys is somewhat larger than that of CePt_2 . Some of this increase could be due to an altered distribution of crystal-field splittings due to disorder. The dis-

order can also affect the phonon spectrum which may account for the rest of the increase. Below 2 K the alloys do not exhibit the large peak seen in the specific heat of CePt_2 , but exhibit a smaller and broader maximum [Fig. 4(b)]. This could mean that the phase transition is subject to substantial inhomogeneity broadening, or that there is no well defined phase transition in the alloys. The specific heat of the alloys is reminiscent of that observed in heavy fermion compounds; it is similar to, though 50% larger than, the specific heat expected⁸ for a set of uncorrelated $S=1/2$ (Γ_7 doublet) Kondo impurities with a Kondo temperature 1.5 K [Fig. 4(b)]. The additional specific heat beyond that expected for the Kondo impurity can be attributed to magnetic correlations in the nonmagnetic heavy fermion ground state.⁹ In any case, the behavior is very different from that expected for a mixed-valent compound, where a much smaller (≈ 50 –100 mJ/mole Ce K^2) linear coefficient of specific heat is expected.

In conclusion, we have confirmed that the CePt_{2+x} alloys have a broad homogeneity range $0 \leq x \leq 1$. Structural refinements with the neutron diffraction data for CePt_3 suggest a preference for the disordered $C15b$ structure over the $C15$ structure with a 95% confidence level. This is corroborated by the existence of small peaks in the diffraction pattern for CePt_3 corresponding to (4,2,0) and (6,0,0) reflections that are forbidden for the $C15$ structure but allowed for the $C15b$ structure. Both imply that $C15b$ is probably the correct structure for this alloy composition, and possibly for the others as well. The susceptibility and specific heat of the alloys are very similar to that of CePt_2 , suggesting that the cerium remains trivalent and localized; they are typical of nonmagnetic heavy fermion compounds with a small characteristic energy (2 K) where the magnetic correlations increase the specific heat somewhat beyond the single ion limit. They are clearly not strongly mixed valent, and hence the photoemission results⁴ cannot be easily explained within the framework of the conventional Kondo lattice theory. The observation of strong mixed valence in Ce 3d core-level XPS studies⁵ of CePt_3 remains a mystery.

Work at Irvine was supported by the UC/LANL INCOR program and by the UC Personnel Assignment Program; work at Los Alamos and Livermore by the U. S. DOE under Contracts Nos. W-7405-ENG-36 and -48, respectively. IPNS is funded as a national users facility by the DMS, OBES/DOE.

¹I. R. Harris, *J. Less-Common Met.* **14**, 459 (1968).

²R. R. Joseph *et al.*, *Phys. Rev. B* **5**, 1878 (1972).

³J. Tang *et al.*, *Phys. Rev. B* **48**, 15 342 (1993).

⁴A. B. Andrews *et al.*, *Phys. Rev. B* **51**, 3277 (1995).

⁵M. Campagna and F. U. Hillebrecht, in *Handbook on the Physics and Chemistry of Rare Earths*, edited by K. A. Gschneidner, Jr., L. Eyring, and S. Hufner (North-Holland, Amsterdam, 1987),

Vol. 10, p. 75.

⁶A. C. Larson and R. B. Von Dreele (unpublished).

⁷J. M. Lawrence *et al.*, *Phys. Rev. B* **54**, 6011 (1996).

⁸V. T. Rajan, *Phys. Rev. Lett.* **51**, 308 (1983).

⁹J. M. Lawrence and D. L. Mills, *Comments Condens. Matter Phys.* **15**, 163 (1991).